CHAPTER 9

Micro Fluid Dynamics in Three-Dimensional Engineered Cell Systems in Bioreactors

M.T. Raimondi*, F. Boschetti, F. Migliavacca, M. Cioffi and G. Dubini

Summary

Bioreactors allowing direct perfusion of culture medium through tissue-engineered constructs may overcome diffusion limitations associated with static culturing, and may provide flow-mediated mechanical stimuli. The hydrodynamic stress imposed on cells in these systems will depend not only on the culture medium flow rate but also on the scaffold three dimensional (3D) micro-architecture. We performed computational fluid dynamics (CFD) simulations of the flow of culture medium through chondrocyte-seeded 3D porous scaffolds, cultured in a direct perfusion bioreactor, with the aim of predicting the shear stress acting on cells adhering on the scaffold walls, as a function of various parameters that can be set in a tissue-engineering experiment. We developed three CFD models: model 1 was built from histological sections of a fibre scaffold, model 2 was built from micro-computed tomography reconstruction of a porous foam, and model 3 was based on an idealized geometry of the actual porous foam. The simulations predicted different distributions of the shear stresses, acting on the scaffold walls, for each scaffold geometry modelled. In contrast, the simulations predicted an identical value of median shear stress in all of the three models. Our results provide a basis for the completion of more exhaustive quantitative studies to further assess the relationship between perfusion, at known micro-fluid dynamic conditions, and tissue growth *in vitro*.

Keywords: tissue engineering, cartilage, bioreactor, shear stress, computational fluid dynamics

*Correspondence to: M.T. Raimondi, Laboratory of Biological Structure Mechanics, Structural Engineering Department, Politecnico di Milano, Milano, Italy. E-mail: manuela.raimondi@polimi.it

Introduction

The generation of autologous cartilaginous grafts requires the development of procedures not only to expand human chondrocytes quickly, but also to promote their re-differentiation in a reproducible way and to maintain their chondrogenic potential in 3D culture systems (1). The conditions which favour *in vitro* chondrogenesis include high cell density and maintenance of spherical cell shape by reduced cell/matrix interaction. This condition may be achieved if the cells are carried by a 3D scaffold, depending on the scaffold material, geometry and pore size (2). Other conditions which are believed to favour *in vitro* chondrogenesis include efficient nutrient delivery and mechanical stimulation (3, 4). Direct perfusion systems may provide an effective strategy to overcome current diffusion limitations associated with culturing 3D tissues *in vitro*, by enhancing nutrient delivery and catabolites removal within the constructs and by providing flow-mediated mechanical stimuli (5-8). However, in most of the direct perfusion systems currently available, the hydrodynamic environment imposed on cells is neither characterized nor controlled. This condition is required to quantify the response to flow-mediated mechanical stimuli of these 3D cell systems.

We developed a direct perfusion bioreactor in which the culture medium flows through porous cellular constructs (9, 10). In this chapter we present CFD models, developed for different scaffolds, of the hydrodynamic environment imposed by such bioreactor. CFD modelling provides a method for relating the flow of culture medium applied to cells on a macroscopic level to the shear stress imposed to the cells on a microscopic level.

Materials and Methods

General description of the computational models

Three CFD models were set up. Model 1 is two-dimensional (2D), models 2 and 3 are three-dimensional (3D). All of the CFD models assume steady flow. The culture medium was modelled as an incompressible, homogeneous, Newtonian fluid with density, ρ, equal to 1000 kg m^{-3}. The viscosity, μ, measured at 37°C by means of a Series 100 capillary viscometer (Cannon-Fenske, State College, PA, USA), was set at $8.2 \bullet 10^{-4}$ kg $m^{-1}s^{-1}$.

The commercial codes used to set up and solve the CFD problems and to analyse the results were all by Fluent (Lebanon, NH, USA). The solid models and meshes were built using GAMBIT; the solvers used were the finite-element code FIDAP for models 1 and 3 and the finite-volume code FLUENT for model 2. All computations were carried out on Windows NT PCs with 512 Mb RAM.

The statistical analysis used to analyze results was based on the element number (% frequency) for models 1 and 3, because the mesh was homogenous. Statistics were based on the element area (% area) for model 2, because the mesh was in-homogenous.

Model 1- fibre scaffold

The first scaffold modelled is Hyalograft 3D (FAB, Abano Terme, PD, Italy), a non-woven mesh made of a benzyl esther of hyaluronic acid. In this particular scaffold, cells were attached to fibres 15 μm in diameter, which were randomly distributed in a 3D space traversed by a constant flow of culture medium (Fig. 1). The cell dimension was assumed to be negligible in this system, if compared to the fibre dimension. The working hypothesis assumed was that the fluid-induced shear stresses acting at the fibre

surfaces represented a realistic estimate of the shear stresses acting on the membranes of the cells. The simplified geometry assumed to set up the CFD model consisted of a two-dimensional domain representing a 400x300 μm^2 cross section of a histological sample of a construct, where a group of fibres were arranged in a cross sectional-like pattern (Fig. 2).

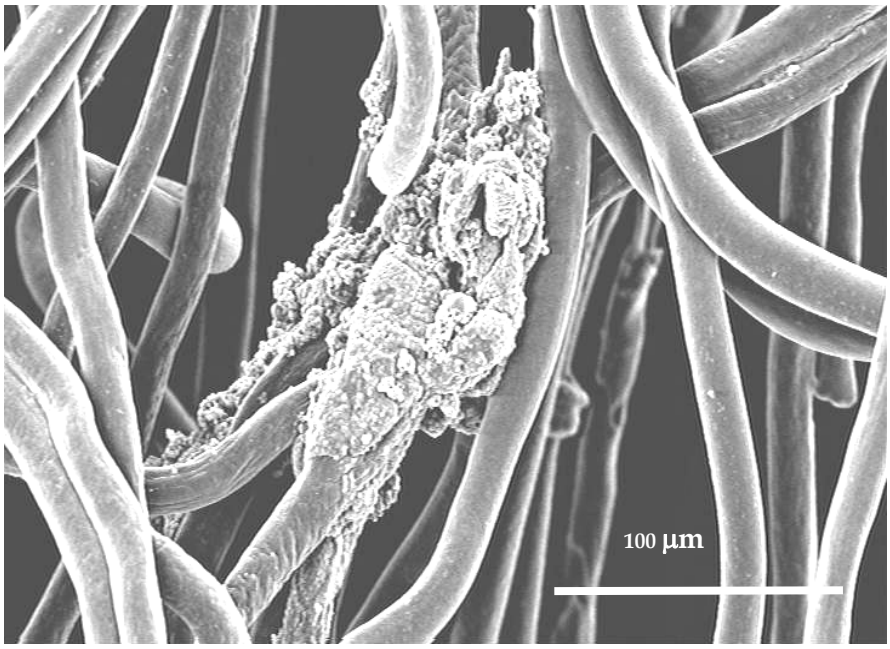

Fig. 1: Scanning electron microscopy image of the fibre scaffold seeded with human articular chondrocytes.

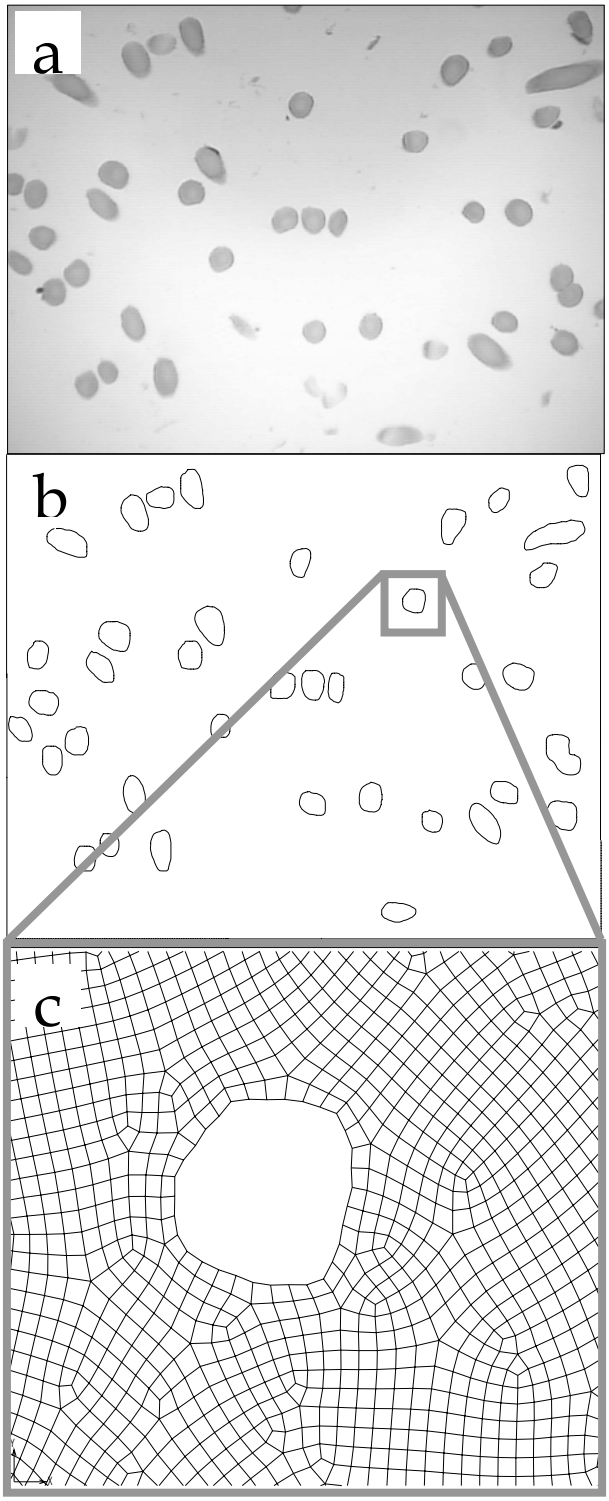

Fig. 2: Method employed to set up model 1: (a) light microscopy image of a cross section of the construct histological sample at original magnification 40x, (b) geometrical definition of the fibres contours and (c) detail of the mesh.

Fourteen light microscopy images of the histological sections were analysed; a representative image is shown in Figure 2a. The geometrical definition of the fibre contours, shown in Figure 2b, was obtained from the images using the Mimics code (Materialise, Leuven, Belgium). The data were then imported as spline curves into the ACIS-based, solid modeller Gambit (Fluent, Lebanon, NH, USA). A paved mesh was used, with a constant interval size of 1.56 μm. Two element types were used: four-node isoparametric quadrilateral elements for the fluid domain and two-node isoparametric edge elements for the fibre contours and the domain contour. The mesh for each image consisted of approximately 52,000 nodes and 56,000 elements, including the edge elements. Mesh and boundary conditions are shown in Figure 5a. No-slip boundary conditions were applied to the fibre contours, under the hypothesis of rigid, impermeable walls. The culture medium flows in from top of the domain and out from bottom. A fully developed laminar flow was obtained at the inlet of the domain by connecting a rectangle, of height approximately equal to ten times the fibre size, to the inlet boundary. A flat velocity profile of 44.2μm/sec was applied at the inlet, corresponding to an average flow rate, Q, of 0.5 $cm^3 min^{-1}$, while null total stress was applied at the outlet. A symmetry boundary condition was used for the lateral sides of the fluid domain (i.e., zero velocity component in the horizontal direction). The Reynolds number was equal to $6.34 \bullet 10^{-4}$.

Post-processing of the CFD results. The shear stresses acting on the fibres contours were extracted from the CFD results. Each image contained a number of fibres ranging from 32 to 66, thus a total of 660 fibres were analysed in the fourteen images. On each fibre contour, the shear stresses vary with the position. Each fibre contour was discretised with about 40 edge elements, on the average, which resulted in more than 26,000 edge elements on the whole. At different flow rate values, the mean shear stress acting on each edge element belonging to a fibre contour, τ, was extracted from the simulation results. The statistical distribution and the median value from all images were determined.

Model 2 – porous foam

The second scaffold modelled is a biodegradable polyestherurethane foam (Degrapol®) with a porosity of roughly 77% and a nominal pore diameter of 100μm. As shown in Figure 3, cells preferentially adhere on the inner surfaces of the scaffold pores; cell dimensions were assumed to be negligible, if compared with the pore size of the foam. The fluid-induced shear stresses acting at the wall surface of the foam were calculated and assumed as an estimate of the shear stresses acting on the membranes of the cells.

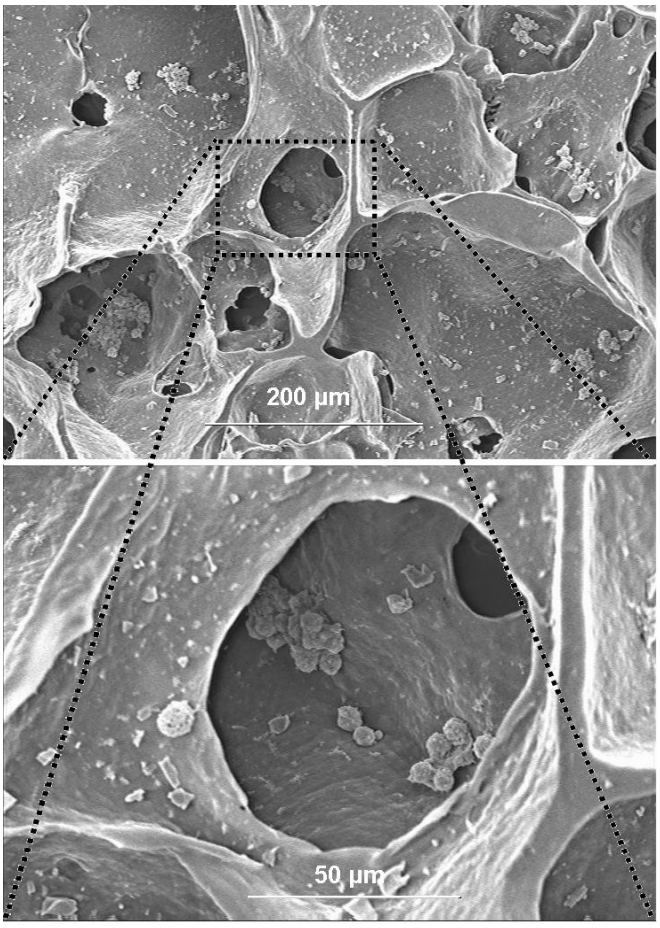

Fig. 3: Scanning electron microscopy image of a porous foam seeded with human articular chondrocytes.

The scaffold micro-geometry was reconstructed from micro computed tomography (μCT) images of the scaffold, acquired using a Skyscan 1072 desk-top x-ray high resolution micro-tomograph (Skyscan, Aartselaar, Belgium). A 1 mm thick sample was acquired in 250 micro-tomograph slices; each slice had a section of 17 mm^2 and a thickness of 4 μm. Tomograph images were stored in BMP files. The methodology for μCT reconstruction is described in detail in Cioffi *et al.* (11).

The 3D model was reconstructed with AMIRA 3.1 software (TGS, San Diego, CA, USA). For each μCT image three sub-areas of the originally measured data were considered, creating three sub-volumes, A, B, C in the central part of the specimen (Fig. 4), to eliminate preparation artefacts on the surface. The three cubes, 400 μm in side, were used separately as geometric models for CFD simulations. The foam was separated from the background with a thresholding procedure, which maintained the scaffold topology. After a smoothing procedure, the fluid volume was visualized by a triangulation of the surface that divided the foam from the void, which would be occupied by the fluid in the CFD simulation. For each cube, the fluid domain was created by meshing the fluid volume in roughly 9,000 tetrahedrons. The mesh of each cube was refined up to reach about 600,000 tetrahedrons for each model. The surface belonging to the central region of each cube (roughly 4,000 faces) was considered as the reference surface for the evaluation of the shear stresses acting on the scaffold walls.

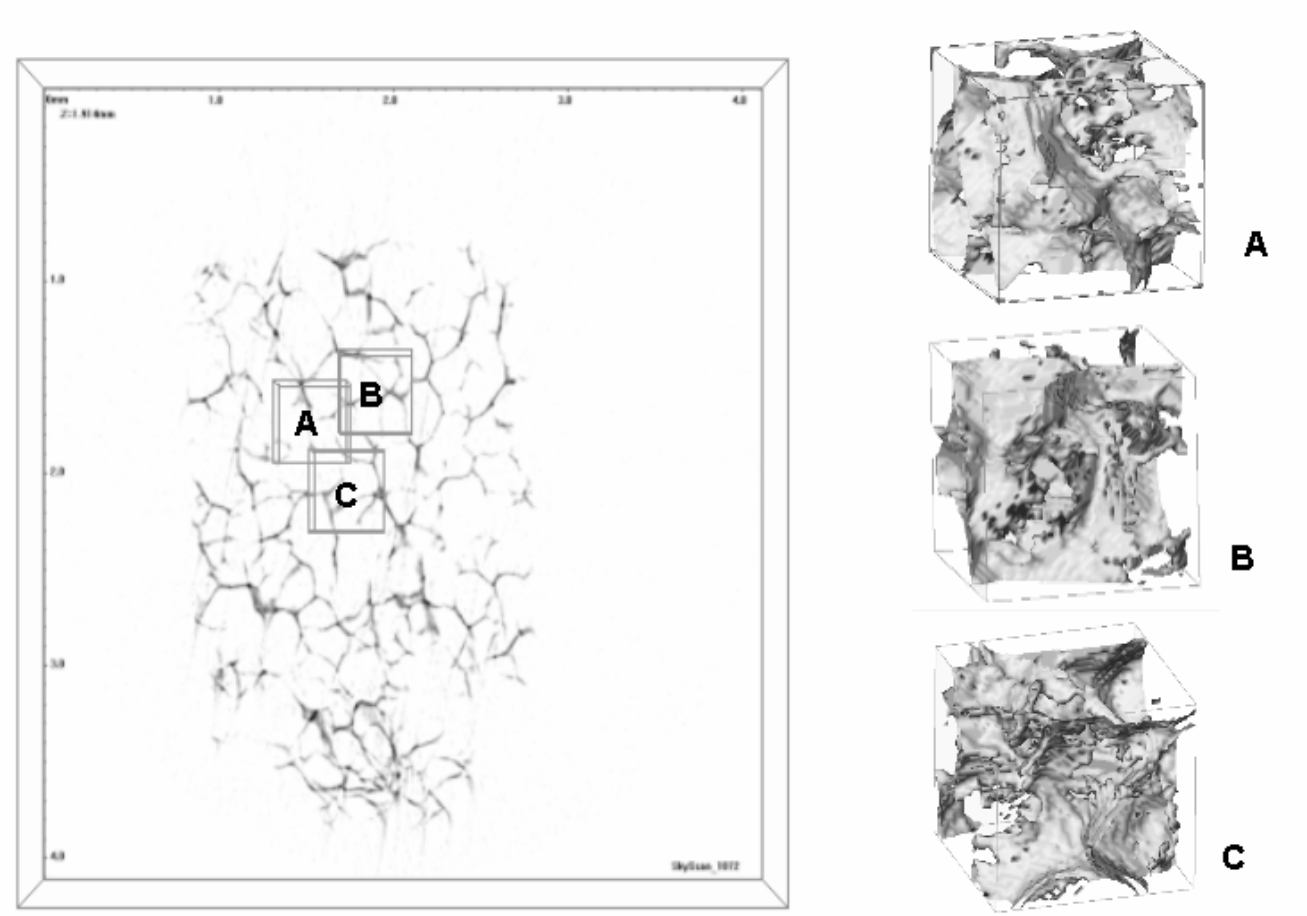

Fig. 4: Method employed to set up model 2: for each micro-CT image, three areas of the originally measured data were considered, to create three volumes of interest, 400 µm in side (cubes A, B, and C), in the central part of the scaffold.

Boundary conditions were set in order to simulate a tissue engineering experiment described in Raimondi *et al.* (10). Mesh and diagram of boundary are shown in Figure 5b. No-slip boundary conditions were applied to the foam surfaces, under the hypothesis of rigid, impermeable walls. The same condition was prescribed to the lateral sides of the fluid domain. The culture medium flows in from the top of the domain and out from the bottom. A flat velocity profile of 53 µm s^{-1} was applied at the inlet,

corresponding to an average flow rate, Q, of 0.5 cm^3 min^{-1} through a porous scaffold of diameter 15 mm, while null total stress was applied at the outlet. The inlet velocity was calculated from the CT images by an estimate of the actual inlet area of the porous scaffold. Further simulations were run for cube A on different values of flow rate (3, 6, and 9 $cm^3 min^{-1}$) in order to investigate the behaviour of the model in various fluid-dynamic conditions. Reynolds number ($Re = d\rho v\mu^{-1}$, d = hydraulic diameter = 4 × volume × surface $area^{-1}$) was equal to 3.42×10^{-4}, 3.71×10^{-4} and 3.70×10^{-4} for cubes A, B and C, respectively.

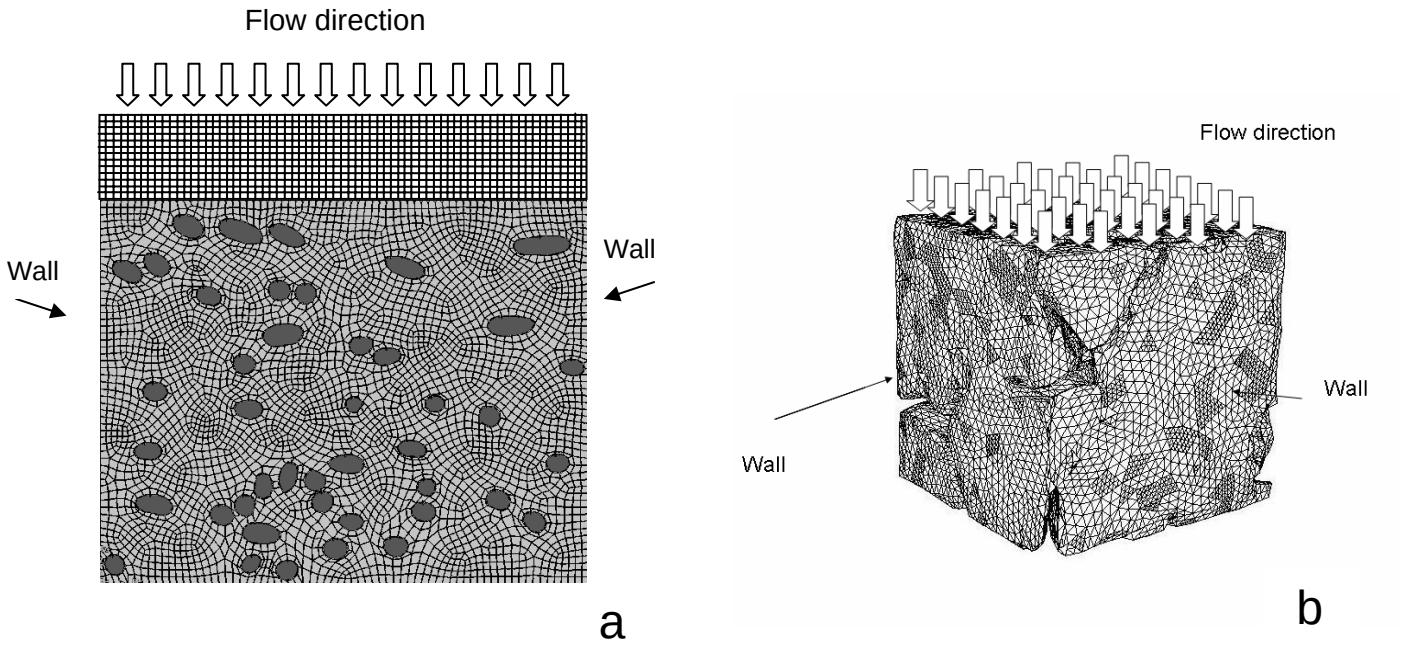

Fig. 5: Mesh and diagram of boundaries for (a) one flow domain of model 1 and (b) one flow domain of model 2.

Post-processing of the CFD results. The fluid induced shear stresses were estracted from the CFD simulations. The surface belonging to the central region of each cube (4,000 faces) was considered as the reference surface for the evaluation of the shear stresses acting on the scaffold walls. For each face the average shear stress was considered. The shear stress values were divided in classes, with a step of 1 mPa, creating approximately 40 classes, from 0 to 40 mPa. The statistical distribution of the shear stress values was considered for each cube (A, B and C), by coupling each shear stress class with the % area with the given shear stress. The mode, mean and median values were calculated. The global statistical distribution of the shear stresses from the three cubes was also created: three groups of faces, their area and their average shear stress were merged together. The mode, mean and median values were again calculated.

Model 3 – idealised porous foam

This CFD model was based on a simplification of the geometry of the polymeric scaffold shown in Figure 3. A micro-domain of the scaffold was idealized as made of 27 sub-units, arranged in a honey-comb-like pattern. Each subunit was obtained by subtracting a solid sphere from a concentric solid cube (Fig. 6).

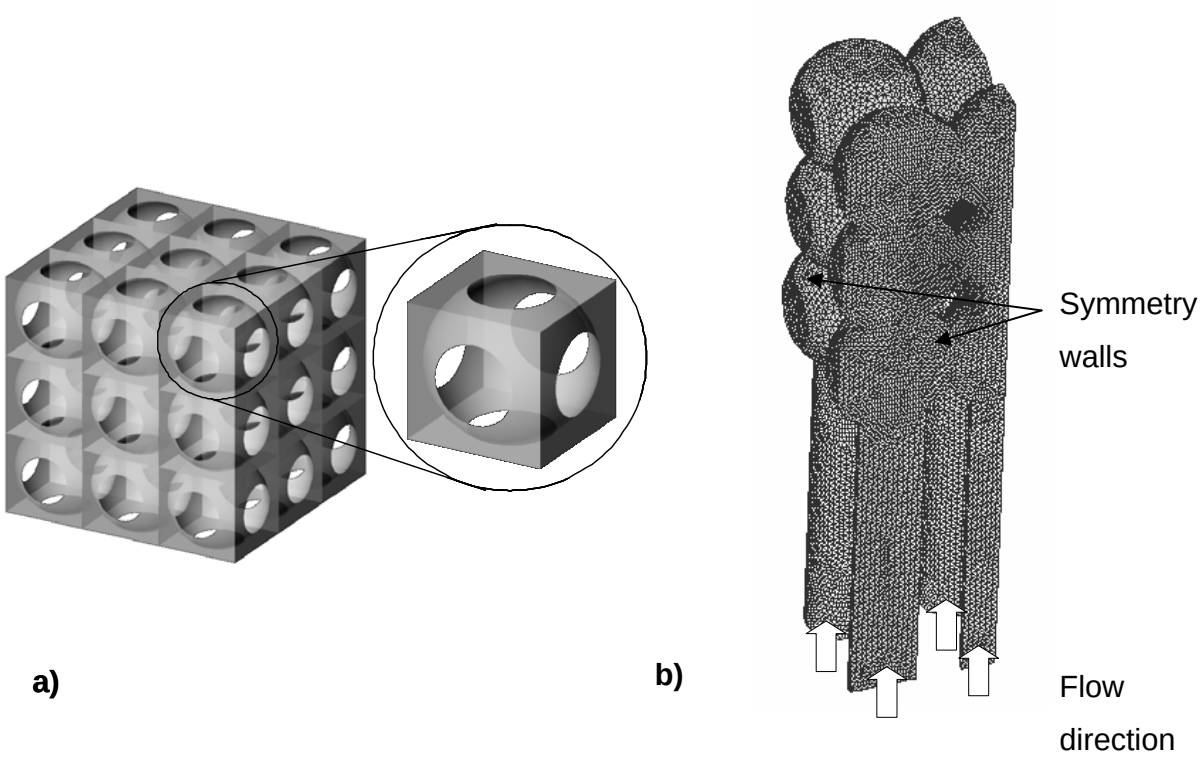

Fig. 6: Method employed to set up model 3: (a) honey-comb structure representing a neighbourhood of a single pore; (b) mesh of the complete domain. The white arrows show the flow direction.

The characteristic lengths of the solid sphere and of the solid cube were varied in order to obtain different pore sizes and porosities, respectively. We built three groups of models corresponding to three diameters of the solid sphere, 50, 100 and 150μm. Each group was made of four models corresponding to 59, 65, 77, and 89% porosity. The porosity was defined as the ratio of void volume to total volume. The reference model had a porosity of 77%, a sphere diameter of 100 μm and a cube dimension of 86.2 μm.

Due to the existing symmetries, only one fourth of the model was studied. A 4 node-tetrahedral mesh was used, with a higher density in correspondence of the central sub-

unit. The meshes presented a number of elements up to 270,000 depending on porosity and pore size, with a corresponding number of nodes up to 50,000.

No-slip boundary conditions were applied to the solid surfaces, under the hypothesis of rigid and impermeable walls. The fluid flows in from the bottom of the domain and out from the top. A fully developed laminar flow was obtained at the inlet of the porous domain by connecting 9 tubes, of length approximately equal to ten times the pore size, to the inlet circles. A flat velocity profile was applied to the tube inlets, while null total stress was applied to the outlet. The inlet velocity was calculated as the ratio of the flow rate, Q, and the area of the inlet section effective to the flow (i.e., the surface area of the inlet section multiplied by the surface porosity) and ranged between 105 and 689 μm/s depending on the porosity. We considered an average flow rate, Q, of 0.5 $cm^3 \bullet min^{-1}$ and a circular scaffold of 15 mm diameter. A symmetry boundary condition was used for the lateral sides of the fluid domain.

The Reynolds number varied between $5 \bullet 10^{-4}$ and $6 \bullet 10^{-2}$, depending on the model geometry. The Reynolds number was calculated as explained above for model 2.

Post-processing of the CFD results. The results of the computations were analysed in the central sub-unit of the honey-comb structure, to avoid boundary effects. The distribution of the shear stress, τ, was determined for the internal walls of the central sub-unit. The number of elements for each central unit ranged between 222 and 689. Shear stress data were processed to obtain the maximum, minimum, average value of τ and its frequency distribution. The frequency distribution was built considering τ intervals of 1 mPa. The mode value of τ is defined as $\tilde{\tau}$ and represents the value of shear stress to which most of the cells adhered to the scaffold walls would be subjected at the beginning of culture. The Reynolds number here is very low, thus the convective terms are negligible and the shear stress is linearly related to the imposed inlet flow rate. Therefore, the calculated shear stresses were used to extrapolate $\tilde{\tau}$ for different flow rates and scaffold sizes.

Results

Model 1- fibre scaffold

The calculated field of velocity and flow streamlines are shown in Figure 7 for a representative image analysed. As one could expect, the volume flow is lower in regions of high fibre concentration, where the resistance to flow is higher. The streamline contours resulting from the simulations clearly show the existence of low flow regions where the fibres are massed and conversely the existence of preferential flow paths. Because of the extremely low Reynolds number, recirculation and separation zones are not present in the domains.

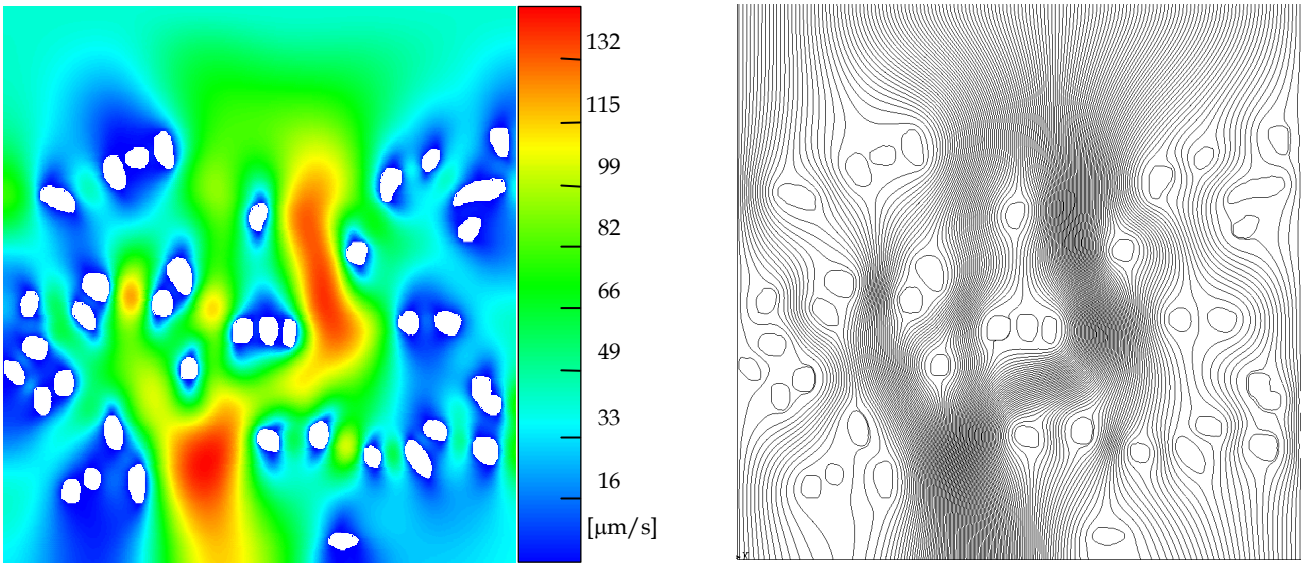

Fig. 7: Results of the CFD simulations for a representative image analysed (model 1); (a) map of velocities and (b) streamlines.

The calculated field of shear stresses is presented in Figure 8 for all the 14 images analysed. As the velocity is zero on the fibre contours, the higher values of shear stress, τ, are localised at the fibre contour segments that face regions of high flow. Due to the unequal distribution of the fibres within the scaffold structure, the values of τ vary considerably not only on each fibre contour, but also among fibres. The distribution of contour shear stresses shows a large spread on low values; however the tail extends up to maximal values on the order of 80 mPa (0.8 dyne/cm^2). The median τ calculated at the fibres contour, at the flow rate of 0.5 cm^3•min^{-1}, corresponding to a 44.2 µm•s^{-1} inlet velocity, is 3 mPa. Model 1 showed a mode value of 1 mPa. The 25th percentile was 1 mPa and the 75th percentile was 11 mPa. The 95th percentile, which gives an estimation of the maximum shear stress, was 80 mPa.

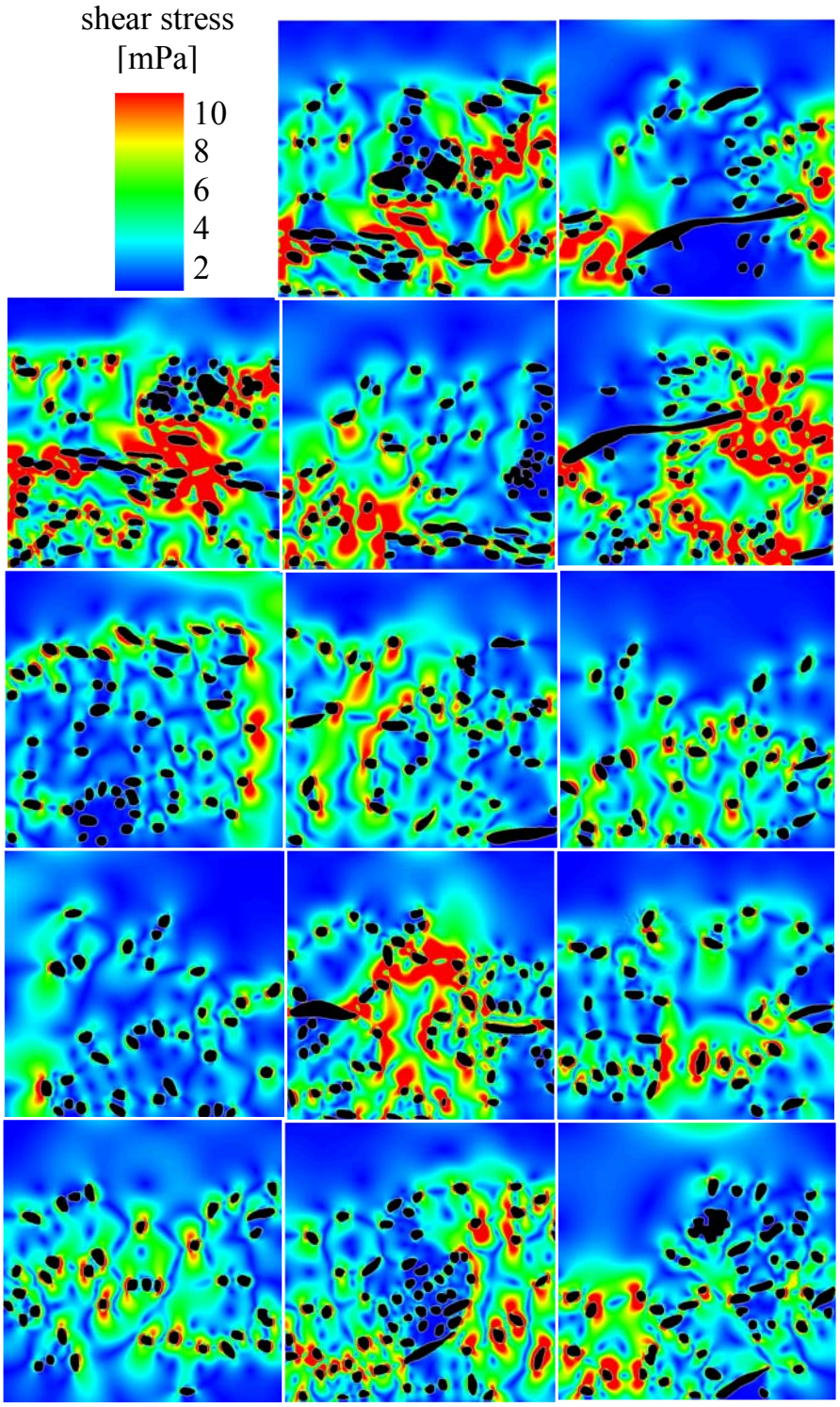

Fig. 8: Results of the CFD simulations for the 14 images analysed (model 1): the shear stress field is mapped for each fluid domain obtained from the histological images.

Figure 9 shows the calculated shear stress values imposed on cells in the direct perfusion bioreactor, as a function of the culture medium flow rate and of the inlet velocity. The median values range linearly ($R^2 > 0.999$) from 0 to 15.3 mPa (0.153 dyne/cm^2) for recirculation flow rates in the range 0 to 2.25 cm^3•min^{-1}, corresponding to inlet velocities ranging from 0 to 200 μm/s. The linear behaviour is consistent with the very low Reynolds number that causes the convective terms in the Navier-Stokes equations to be negligible.

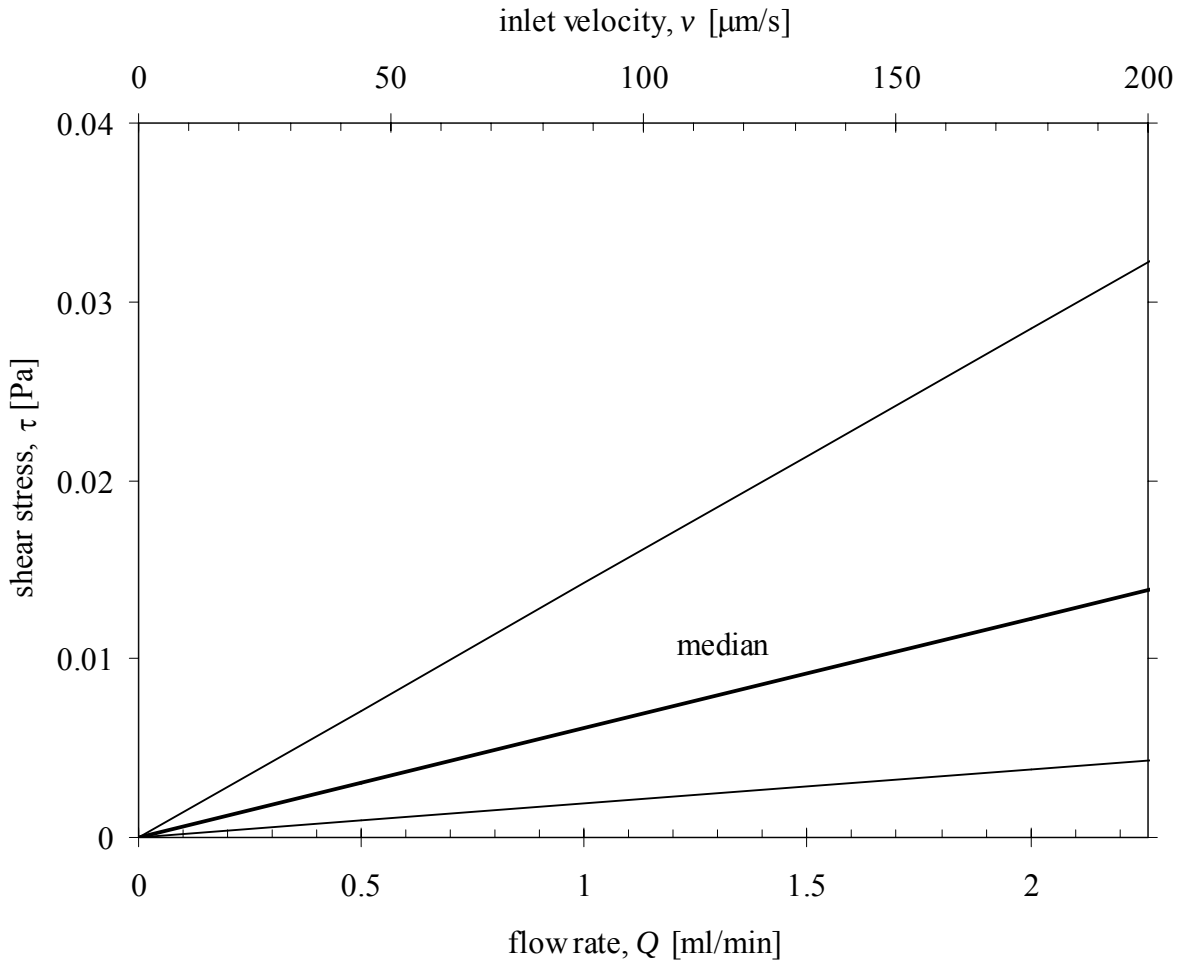

Fig. 9: Extrapolation of results from CFD simulations (model 1): calculated shear stress level imposed on cells in the direct perfusion bioreactor, as a function of the culture medium flow rate and of the inlet velocity. The light lines represent the 25th and the 75th percentiles of the calculated shear stress distribution.

Model 2 – porous foam

The computed fluid dynamic field was found to be strongly affected by boundary effects. For this reason, wall shear stress values were evaluated for the inner surface of each cubic sub-model. Figure 10 shows the wall shear stresses mapped on the considered area.

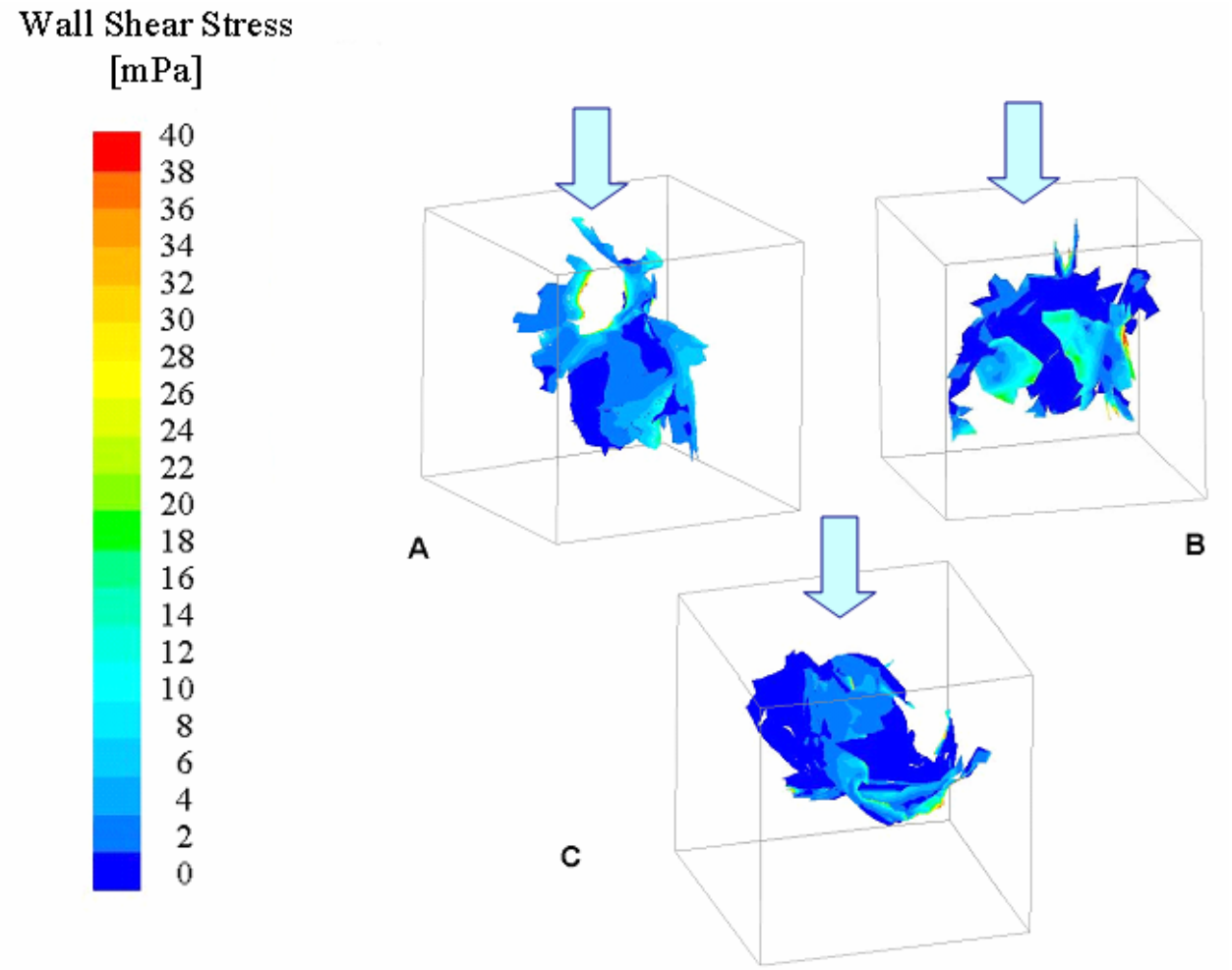

Fig. 10: Results of the CFD simulations (model 2): the wall shear stress field is mapped on the inner surface for three cubic sub-volumes obtained from the μCTs.

The wall shear stress distribution was calculated for the inner area of each model: here, the shear stress varies between 0 and 40 mPa among 95% of the surface in the domain. The mode and the median value range from 2 to 4 mPa for the three models. The global distribution of the sum of the three cubic sub-models shows a median value of 3 mPa. The 25th percentile was 2 mPa for all the cubes (A, B and C). The 75th percentile was 10 mPa, 12 mPa and 9 mPa for cube A, B and C respectively. The 95th percentile was 39 mPa, 42 mPa and 38 mPa for cube A, B and C respectively. The global statistical distribution of the shear stresses (cubes A+B+C) had a median shear stress of 3 mPa and a mode value of 2 mPa. The 25th percentile was 2 mPa, the 75th percentile was 10 mPa, the 95th percentile was 40 mPa.

The mean shear stress ranges linearly from 0 to 71 mPa, for flow rates in the range of 0 to 9 $cm^3 \cdot min^{-1}$, corresponding to inlet velocities of 0 to 954 μms^{-1}. The shear stress distribution slightly changes for high values of imposed flow rate, showing a median τ value of 15, 20, and 45 mPa for flow rates of 3, 6 and 9 $cm^3 \cdot min^{-1}$, respectively.

Model 3 – idealised porous foam

The shear stress distributions on the walls of the central pore are mapped in Figure 11 for all the porosities and pore sizes modelled.

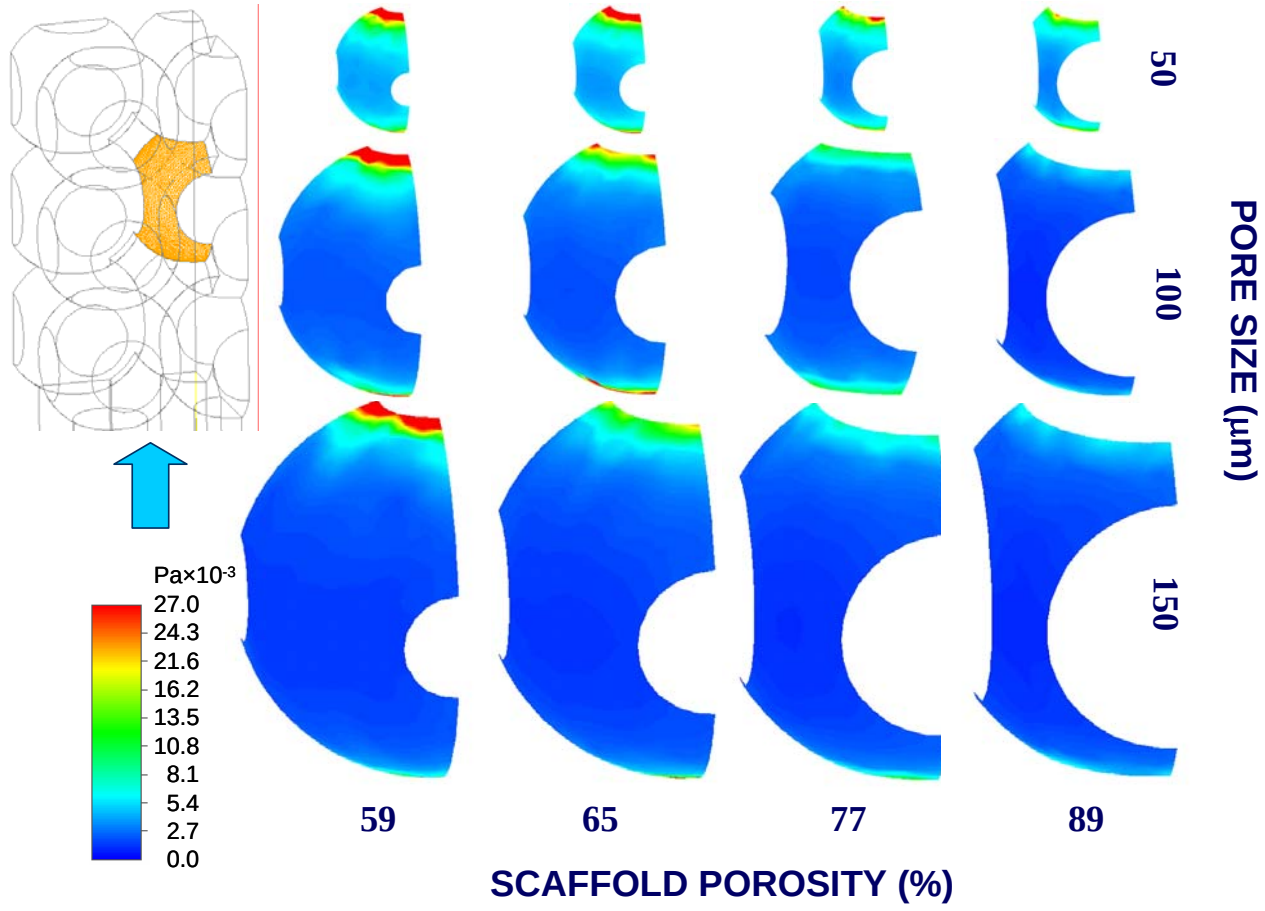

Fig. 11: Results of the CFD simulations (model 3): the wall shear stress field is mapped on the inner surface of the central pore, at increasing porosity and pore dimension.

Although the shear stress, τ, reaches values up to 70 mPa at the pore inlet and outlet, the shear stress acting on most of the pore wall is much lower, generally around 3 mPa. For increasing porosities, the calculated mode, $\tilde{\tau}$, is roughly constant, whereas the stress distribution spreads, consistently with the presence of smaller wall areas subject to uniform stresses. In contrast, for increasing pore size, the values of $\tilde{\tau}$ decrease, consistently with the presence of lower velocity gradients, while the stress distribution narrows, consistently with the presence of larger wall areas subject to uniform stresses. All the above results were obtained for a circular scaffold, 15 mm in diameter, perfused by a flow rate of 0.5 $cm^3 \bullet min^{-1}$. The mode and the median value were 3 mPa. The 25th and 75th percentile were 2 mPa and 4mPa respectively. The 95th percentile was 11 mPa.

The values of τ extrapolated for other scaffold diameters and flow rates are plotted in Figure 12. Here, the ratio $\tilde{\tau}/Q$, is given as a function of the diameter of the perfused section, D, for different values of pore diameter. The porosity is not accounted for as it does not affect $\tilde{\tau}$, as stated above.

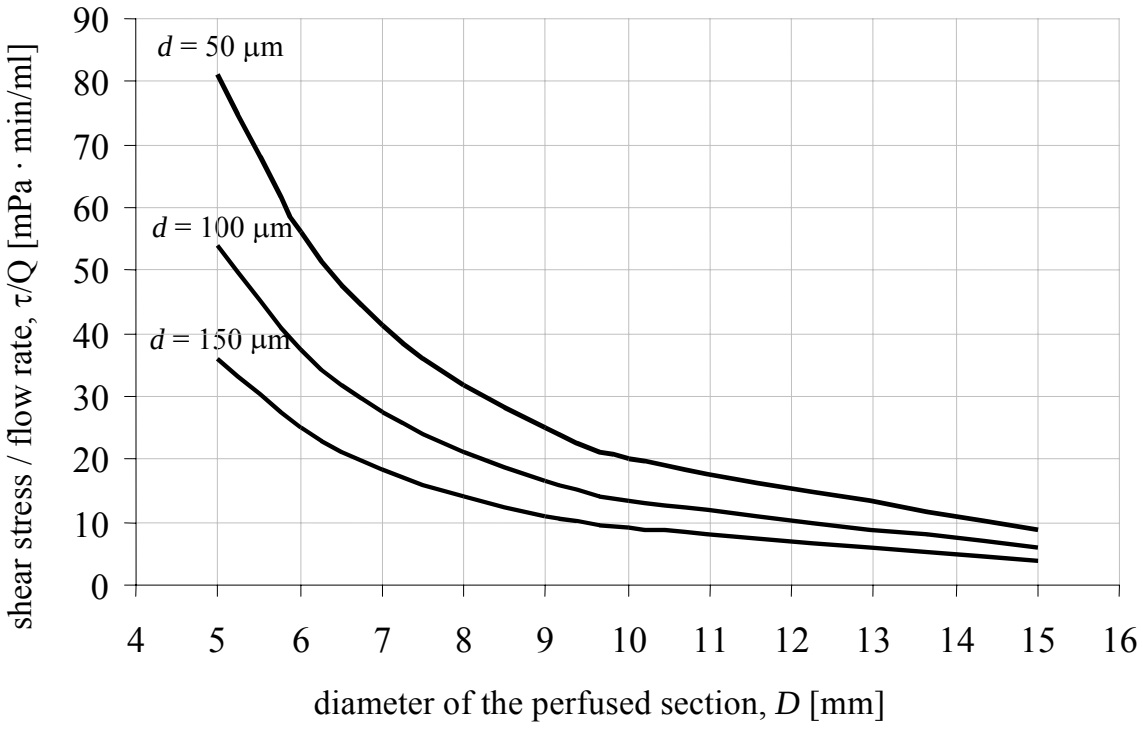

Fig. 12: Shear stress level imposed on cells in the direct perfusion bioreactor, extrapolated from the results of model 3, normalised by the flow rate, as a function of the diameter of the perfused section, D, for different values of pore diameter, *d*.

Discussion

The target of the studies here described was to characterise the hydrodynamic field imposed on cells in cellular constructs cultured in a direct perfusion bioreactor. The CFD simulations numerically predicted the shear stresses induced at the internal walls in relation to three scaffold geometries.

In fibre scaffolds, configured as the ones represented in Figure 1, cells adhere preferentially at the fibre intersections. The fibres are randomly massed, thus cells are often located in regions of lower flow, where the shear stresses predicted by the simulations showed a spread on low values. The most severe simplification in our model 1 was the 2D flow modelling. Since the fibres appear in a cross sectional view, the computed fluid dynamics are that typical of a bank of tubes in cross flow, randomly staggered. In such a configuration the fibre axes extend infinitely in the direction normal to the plane of the model. Results from models 2 and 3 indicated that an open-pore structure, rather than a fibre structure, is likely to optimise hydrodynamic stimulation and mass transport to the cells.

Although the three models represented different geometries, they all predicted the same level of median shear stress. This implies that at very low Reynolds numbers, the actual micro-geometry of the scaffold does not significantly affect the level of shear stress acting on the inner scaffold walls. Thus, simplified models may correctly predict the level of shear stress imposed on cells adhering to the scaffold walls. In contrast with this finding, the simulations showed a great variability of results between the three scaffolds modelled, in terms of distribution of the shear stresses. This variability can be explained by the great differences in microgeometry among the three modelled scaffolds. In the case of an irregular geometry (models 1 and 2) the stress distribution spreads, consistently with the presence of smaller wall areas subject to uniform stresses. In

contrast, for a microstructure showing a regular geometry (model 3), in specific conditions the simulations showed a very narrow stress distribution.

These results can be used to derive new scaffold design criteria. For example, indication on microstructures in which the hydrodynamic field imposed on cells is optimised against specific flow parameters.

Acknowledgments

This research is supported by Fondazione Cariplo and by Politecnico di Milano (grant CelTec). The porous foams were supplied without charge by ETH (Zurich, CH). The μCT equipment was made available without charge c/o Istituto Ortopedico Rizzoli (Bologna, Italy) by the company Assing (Monterotondo, Roma, Italy), the equipment was operated by Dr. Egon Perilli. The cell cultures were performed at Niguarda Hospital in Milano.

References

1. Jakob M, Demarteau O, Schafer D, Hintermann B, Dick W, Heberer M, Martin I. Specific growth factors during the expansion and redifferentiation of adult human articular chondrocytes enhance chondrogenesis and cartilaginous tissue formation in vitro. J Cell Biochem 2001; 81:368-377.
2. Hutmacher DW. Scaffolds in tissue engineering bone and cartilage. Biomaterials 2000; 21:2529-2543.
3. Ingber DE. Mechanochemical switching between growth and differentiation by extracellular matrix. Lanza RP, Langer R, Chick WL, editors. Principles of tissue

engineering. Houston, Texas: R.G. Landes Company and Academic Press, Inc.; 1997:89-100.

4. Martin I, Obradovic B, Treppo S, Grodzinsky AJ, Langer R, Freed LE, Vunjak-Novakovic G. Modulation of the mechanical properties of tissue engineered cartilage. Biorheology 2000; 37:141-147.
5. Dunkelman NS, Zimber MP, LeBaron RG, Pavelec R, Kwan M, Purchio AF. Cartilage production by rabbit articular chondrocytes on polyglycolic acid scaffolds in a closed bioreactor system. Biotechnol Bioeng 1995; 46:299-305.
6. Pazzano D, Mercier KA, Moran JM, Fong SS, DiBiasio DD, Rulfs JX, Kohles SS, Bonassar LJ. Comparison of chondrogensis in static and perfused bioreactor culture. Biotechnol Prog 2000; 16:893-896.
7. Mizuno S, Allemann F, Glowacki J. Effects of medium perfusion on matrix production by bovine chondrocytes in three-dimensional collagen sponges. J Biomed Mater Res 2001; 56:368-375.
8. Davisson T, Sah RL, Ratcliffe A. Perfusion increases cell content and matrix synthesis in chondrocyte three-dimensional cultures. Tissue Eng 2002; 8:807-816.
9. Raimondi MT, Boschetti F, Falcone L, Fiore GB, Remuzzi A, Marazzi M, Marinoni E, Pietrabissa R. Mechanobiology of engineered cartilage cultured under a quantified fluid dynamic environment. Biomech Model Mechanobiol 2002; 1:69-82.
10. Raimondi MT, Boschetti F, Falcone L, Migliavacca F, Remuzzi A, Dubini G. The effect of media perfusion on three-dimensional cultures of human chondrocytes: integration of experimental and computational approaches. Biorheology 2004; 41:401-410.
11. Cioffi M, Boschetti F, Raimondi MT, Dubini G. Modeling evaluation of the fluid-dynamic microenvironment in tissue-engineered constructs: A micro-CT based model. Biotechnol Bioeng 2006; 93:500-510.

CHAPTER 9

Micro Fluid Dynamics in Three-Dimensional Engineered Cell Systems in Bioreactors

M.T. Raimondi*, F. Boschetti, F. Migliavacca, M. Cioffi and G. Dubini

Summary

Bioreactors allowing direct perfusion of culture medium through tissue-engineered constructs may overcome diffusion limitations associated with static culturing, and may provide flow-mediated mechanical stimuli. The hydrodynamic stress imposed on cells in these systems will depend not only on the culture medium flow rate but also on the scaffold three dimensional (3D) micro-architecture. We performed computational fluid dynamics (CFD) simulations of the flow of culture medium through chondrocyte-seeded 3D porous scaffolds, cultured in a direct perfusion bioreactor, with the aim of predicting the shear stress acting on cells adhering on the scaffold walls, as a function of various parameters that can be set in a tissue-engineering experiment. We developed three CFD models: model 1 was built from histological sections of a fibre scaffold, model 2 was built from micro-computed tomography reconstruction of a porous foam, and model 3 was based on an idealized geometry of the actual porous foam. The simulations predicted different distributions of the shear stresses, acting on the scaffold walls, for each scaffold geometry modelled. In contrast, the simulations predicted an identical value of median shear stress in all of the three models. Our results provide a basis for the completion of more exhaustive quantitative studies to further assess the relationship between perfusion, at known micro-fluid dynamic conditions, and tissue growth *in vitro*.

Keywords: tissue engineering, cartilage, bioreactor, shear stress, computational fluid dynamics

*Correspondence to: M.T. Raimondi, Laboratory of Biological Structure Mechanics, Structural Engineering Department, Politecnico di Milano, Milano, Italy. E-mail: manuela.raimondi@polimi.it